ISSN 2959-6157

Research on the influencing factors of the difference in warming rates between the east, west and central regions of North America during the 21st century

Ruyun Xie[1,a,#], Yunbo Zhao[1,b,#], Xinlin Ni[1,c,#,*], Wenlan Cui[2,d]

[1]University of Reading, Reading RG6 6AH, United Kingdom
[2]Acabridge Academic, Shanghai 200065, China.
[a]gw804943@student.reading.ac.uk,
[b]yb804685@student.reading.ac.uk,
[c*]ud804806@student.reading.ac.uk,
[d]3599742790@qq.com
[#]co-first authors
[*]corresponding author

Abstract:

Temperature in North America (NA) is a significant focus of current climate change research. This study focuses on various climate variables and employs linear regression and correlation coefficient analysis to examine the factors influencing the differences in warming rates across the eastern, western, and central regions of NA in the 21st century, as well as the correlations between these factors and temperature. Results indicate that NA temperatures are rising with notable regional variations in warming rates. Under the influence of cloud cover, the impact of precipitation on warming rates is relatively minor, whereas radiation significantly affects warming rates. Additionally, sea level pressure influences wind patterns, thereby significantly impacting warming rates. This study highlights the complexity of regional climate dynamics in NA and provides deep insights into regional climate differences.

Keywords: North America (NA); Warming rate; Clouds; Precipitation; Radiation; Sea level pressure; Wind; Correlation.

1. Introduction

Since the pre-industrial era (1850-1900), the global average surface temperature has increased by approximately 1°C. This seemingly minor increase signifies a substantial accumulation of heat. The Sixth Assessment Report of the IPCC (2022) indicates that since 1960, the trend of rising annual average temperatures across North America (NA) has been widespread but uneven[1].

Therefore, this study will analyze climate data to identify the factors contributing to the warming rates across NA, aiming to understand the regional variability of climate change.

Currently, with rising temperatures, extreme heat records in NA are occurring more frequently than extreme cold records [2]. The extent of snow cover has decreased in much of Canada and the western United States [3]. Over the past half-century, glaciers have been retreating in high-altitude regions of NA [4]. Lake ice in Canada, south of the Arctic region, has diminished [5]. In the southwestern deserts of NA, summer daily maximum temperatures are increasing [6]. The IPCC (2021) report indicates a rise in sea level around NA's coastlines[7]. The lack of warming in the central United States, referred to as the "warming hole", is related to regional surface-atmosphere interactions and may lead to increased precipitation, thereby enhancing surface moisture and reducing daytime maximum temperatures [8]. NA accounts for approximately one-quarter of global greenhouse gas (GHG) emissions, with GHG emissions in NA increasing by nearly 18% since 1990 [9]. Carbon dioxide (CO_2) is a major driver of climate change (IPCC, 2021)[7]. In this context, numerous studies have discussed the factors influencing temperature variations. Research suggests that changes in cloud cover and precipitation may influence temperature trends in NA, as NA's summer temperature variations are related to changes in solar heating and surface latent heat

[10]. There is a connection between summer temperature trends in NA and variability in sea surface temperatures (SSTs) [11]. In the southeastern United States, there is a strong negative correlation between summer daily maximum temperatures and precipitation. Moist surfaces may contribute to the stagnation of summer warming in the southern United States, indicating that surface moisture is a significant local factor affecting changes in average daily maximum temperatures during the summer [12]. From 1960 to 1990, despite a decrease in incoming shortwave radiation, land temperatures increased by 0.4°C due to an increase in downward longwave radiation, suggesting that surface energy balance is a key process controlling land temperature evolution [13]. Atmospheric circulations such as the El Niño–Southern Oscillation (ENSO) can also affect summer temperatures in NA [14].

However, existing research lacks analysis of temperature changes and influencing factors in NA over the past two decades. More research has focused on differences in temperature values, with little attention paid to variations in temperature trends across different regions of NA. In terms of influencing factors, the emphasis has been primarily on precipitation, summer cloud cover, and radiation, with scant investigation into the trend changes of other factors, such as precipitation, average cloud cover, and radiation, and their impact on temperature. Additionally, while there has been considerable focus on the effects of these factors on NA's summer maximum temperatures, there is a notable absence of studies examining their impact on the average temperature trend rate.

Therefore, this study selected a time scale of nearly 24 years for analysis. Focus on the impact of average cloud cover, precipitation, radiation amount, sea level pressure, wind change and other trends on the average temperature trend rate in different regions of NA. Additionally, it aims to determine the extent to which these factors influence the average temperature trend rate in different regions and to explore the relationships between these influencing factors.

2. Data & Methods

2.1 Data

2.1.1 Satellite Data

Utilizing the data from the Clouds and Earth's Radiant Energy Systems - Energy Balanced and Filled (CERES-EBAF) Ed4.1 version (https://ceres-tool.larc.nasa.gov/ord-tool/jsp/EBAFTOA42Selection.jsp, last accessed: 17 July 2024), we conducted an in-depth analysis[15], [16]. These datasets provide monthly averaged information on shortwave, longwave, and net radiation at the top of the atmosphere (TOA), with a spatial resolution of 1° x 1° grids, accompanied by imager data on cloud properties. In our study, we primarily focused on the temporal and spatial variations of these parameters and calculated their trends to identify their correlation with temperature warming in NA. The data span covers the period from March 2000 to December 2023.

The Global Precipitation Climatology Project (GPCP) precipitation product, version V2.3, was also employed (https://psl.noaa.gov/rest/data.gpcp.html, last accessed: 22 July 2024) [17]. In GPCP, data from rain gauge stations, satellites, and sounding observations have been integrated to estimate the Average Monthly Rate of Precipitation on a 2.5-degree global grid. Similarly, our primary focus in this context is on North America and the period since the 21st century.

2.1.2 Reanalysis Data

In order to further study the influence, we also used National Centres for Environmental Prediction-National Centre for Atmospheric Research (NCEP-NCAR) Reanalysis 1 dataset (https://psl.noaa.gov/rest/data.ncep.reanalysis.html, last accessed: 22 July 2024). In this dataset, we mainly used 2m of air temperature, sea level pressure, and potential height (500hPa and 850hPa) data. These data are all monthly average data with a spatial resolution of 2.5°×2.5° and a time scale of 01/2000-12/2023.

Then, we utilized the wind speed data (u-component and v-component) from the fifth generation European Centre for Medium-Range Weather Forecasts (ECMWF) reanalysis (ERA5) (https://cds.climate.copernicus.eu/cdsapp#!/dataset/reanalysis-era5-pressure-levels-monthly-means?tab=form, last accessed: 23 July 2024)[25]. This reanalysis integrates model data with observation data from all over the world into a comprehensive and coherent global dataset through data assimilation. The wind speed data are also presented as monthly averages on isobaric surfaces such as 500hPa and 850hPa. They have a high spatial resolution of 0.25° x 0.25° grids, with a same temporal range.

In addition, we also used the temperature anomaly data in the NASA Goddard Institute for Space Studies (GISS) Surface Temperature Analysis version 4 (GISTEMP v4) (https://data.giss.nasa.gov/gistemp/, last accessed: 17 July 2024). This data comes from NASA, which is updated around the middle of every month using current data files from National Oceanic and Atmospheric Administration (NOAA) Global Historical Climatology Network (GHCN) v4 (meteorological stations) and Extended Reconstructed Sea Surface Temperature (ERSST) v5 (ocean areas) [18], [19]. The spatial resolution of GISTEMP is 2.0°×2.0°, and the time series is also from January 2000 to December

2023.

2.2 Method

2.2.1 Trend Regression Feature

In our research, we primarily utilize the simple linear regression equation to calculate the relationship between two correlated variables, with the target variable denoted as y_i and the feature variable denoted as x_i. Regression analysis is employed to identify the mathematical model y=f(x), and when y=f(x) is a linear equation, it is referred to as simple linear regression. The equation is given by:

$$y_i = \beta_1 x_i + \beta_0$$

Where 'β_0' is the intercept term (or offset), and 'β_1' is the coefficient of the feature variable. Their calculation formulas are:

$$\beta_1 = \frac{n\sum xy - \sum x \sum y}{n\sum\left(x^2\right) - \left(\sum x\right)^2}$$

$$\beta_0 = \frac{\sum y - \beta_1 \sum x}{n}$$

Where 'n' represents the total number of samples.

Then, we determine the values of β_0 and β_1 from the sample data using the method of least squares. The least squares approach is employed to estimate the model parameters by minimizing the sum of squares of all prediction errors. For a given dataset (x_i, y_i), the objective is to find the values of β that minimize the sum of squared errors. The formula for the sum of squared errors (loss function) is:

$$J(\beta) = \sum_{i=1}^{m} (y_i - \widehat{y_i})^2 = \sum_{i=1}^{m} (y_i - (\beta_1 x_i + \beta_0))^2$$

Where 'y_i' is the actual value; '$\widehat{y_i}$' is the model prediction value

In this paper, we first use time (unit: year) as the feature variable and temperature along with various influencing factors as the target variables to calculate their trends over the time series. Subsequently, we compute the correlation between temperature and different influencing factors, with the influencing factors serving as the feature variables and temperature as the target variable. Throughout this process, we derive the coefficient β_1, which is used to compare the importance of different influencing factors. Additionally, we obtain the R-squared value, which describes the proportion of the variation in the target variable that is explained by the feature variables in the model. The function of R^2 is:

$$R^2 = 1 - \frac{\sum (y_n - \hat{y}_n)^2}{\sum \left(y_n - \bar{y}\right)^2}$$

where '$\bar{y}$' is the average value of all actual values y_i.

2.2.2 Correlation Test

Apart from the coefficient β_1, we also employ the Pearson correlation coefficient (PCCs), also known as the Pearson product-moment correlation coefficient (PPMCC), to compare the strength of correlation between different variables. The PCC measures the linear correlation between two variables, X and Y, with values ranging from -1 to 1. A coefficient of 1 indicates a perfect positive correlation between the two variables, -1 indicates a perfect negative correlation, and 0 indicates no linear correlation between the variables. The formula for calculating the Pearson correlation coefficient is:

$$r = \frac{\sum_{i=1}^{n}\left(X_i - \bar{X}\right)\left(Y_i - \bar{Y}\right)}{\sqrt{\sum_{i=1}^{n}\left(X_i - \bar{X}\right)^2 \sum_{i=1}^{n}\left(Y_i - \bar{Y}\right)^2}}$$

2.3 Study Area

This study selects climate data from the NA region between 2000 and 2023 for analysis, with a particular focus on temperature variations in the eastern and western coasts, as well as the central region. From a geographical perspective (Fig 1(a)), NA boasts a vast territory, stretching from the Arctic to tropical regions, bordered by the Pacific Ocean to the west and the Atlantic Ocean to the east, contributing to significant climatic diversity within the region. Furthermore, major cities such as New York, Washington D.C., Chicago, Toronto, and Ottawa are concentrated in the eastern coast, while Los Angeles and San Francisco dominate the western coast, resulting in high population densities in both coastal regions. This causes that 80% of the US population resides in the eastern coast. In contrast, the central region is sparsely populated with lower density, primarily serving as a major agricultural area, creating a stark contrast with the coastal regions.

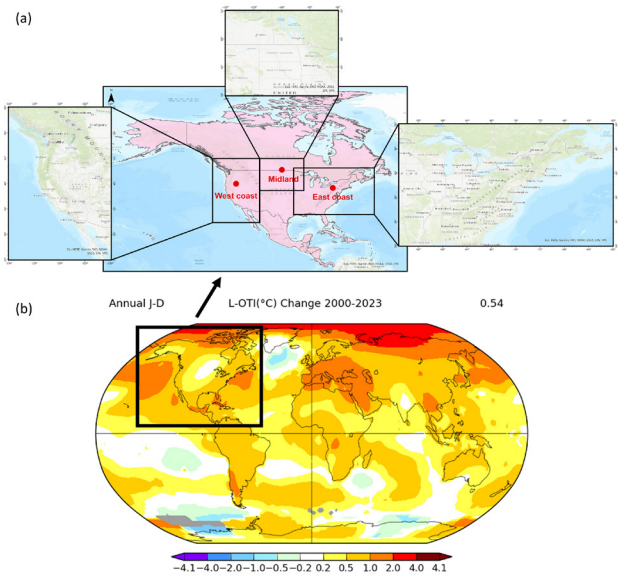

Fig.1 (a) Map of North America (5°N-85°N, 55°W-170°W). West coast region (25°N-55°N, 110°W-130°W); East coast region (30°N-50°N, 60°W-95°W); Central region (40°N-55°N, 90°W-110°W). (b) The trend of the global temperature anomaly (K), the anomaly is based on 1951-1980. Download from the website of National Aeronautics and Space Administration (NASA) (https://data.giss.nasa.gov/gistemp/maps/, last accessed: 12 August 2024).

The Fig 1(b) reveals differing rates of temperature increase between the three regions of NA. Consequently, investigating the factors influencing climate change in these areas holds significant research value.

3. Results & Discussion

3.1 Time Scale

Fig.2 indicates that although there were fluctuations in the average temperature between 2000 and 2023, an overall upward trend is evident (Fig.2(a)). Moreover, the temperature anomalies are all greater than 0 (Fig.2(b)), which further proves the increase in temperature in recent years. This is consistent with the result of the temperature increasing trend mentioned in the IPCC report [1].

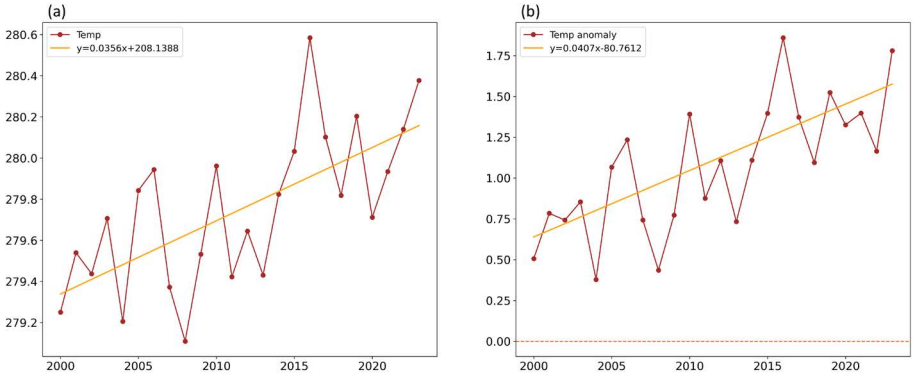

Fig.2 The line graph of (a) average temperature (K) and (b) average temperature anomaly (K) of NA, the anomaly is based on 1951-1980. Data were collected between 2000 and 2023. The orange straight line in the figure represents the fitted trend line.

3.2 Spatial Scale

Fig.3(a) apparent that all the anomalies within this region are all greater than 0, indicating that the average temperature from 2000 to 2023 is higher than that of 1951-1980, showcasing climate warming. Moreover, the temperature increase varies across different regions. Specifically, the temperature rise is more pronounced over land than over oceans, and in high latitudes compared to mid-low latitudes. This confirms the conclusion of significant polar amplification of warming in high-latitude regions of NA [20] and the further reduction of polar sea ice [21].

The trend values within this region are all greater than 0 (Fig.3(b)), indicating a consistent upward trend in temperature. However, the rates of warming vary across different regions. Specifically, the central region exhibits the slowest rate of warming (+0.0081), forming a “warm hole”. Additionally, the trend shows that the western coast (+0.0285) experiences a lower rate of temperature increase compared to the eastern coast (+0.0345) of NA, aligning with the findings of Greenan (2018) [22] and Pan (2004) [8].

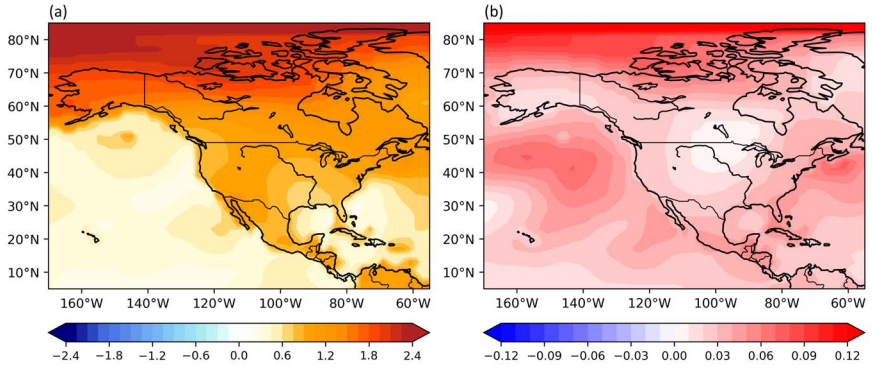

Fig.3 (a) The spatial distribution of the average temperature anomaly (K) in NA from 2000 to 2023, based on 1951-1980. (b) The spatial distribution of the trend of temperature anomaly (K/year) in NA from 2000 to 2023. The trend is the slope calculated by the simple linear regression.

Combining Fig.3(a) and 3(b) reveals that regions with faster warming rates (the northeastern coast of NA) have actually experienced higher temperature increases than regions with slower warming rates (the northwestern coast of NA), which indicates that there is a consistent trend between the warming rates and the actual temperature increases in these two areas. Regions with slower warming rates (the southwestern coast of NA) have actually recorded higher temperature increases than regions with faster warming rates (the southeastern coast of NA), which may be due to the regions experiencing slower warming rates from 2000 to 2023 might have had faster warming rates prior to 2000, resulting in higher baseline temperatures by that year.

3.3 Influence Factors

3.3.1 Cloud & Precipitation

From 2000 to 2023, the NA West Coast exhibited lower and decreasing cloud cover throughout the day, whereas the East Coast experienced higher and increasing cloud cover (Fig.4(a) and 4(b)). Similarly, the NA West Coast had lower and decreasing average precipitation, while the East Coast showed higher and increasing average precipitation (Fig.4(c) and 4(d)), which is similar to the results of Tang(2013) [12] and Zhang(2019) [23].

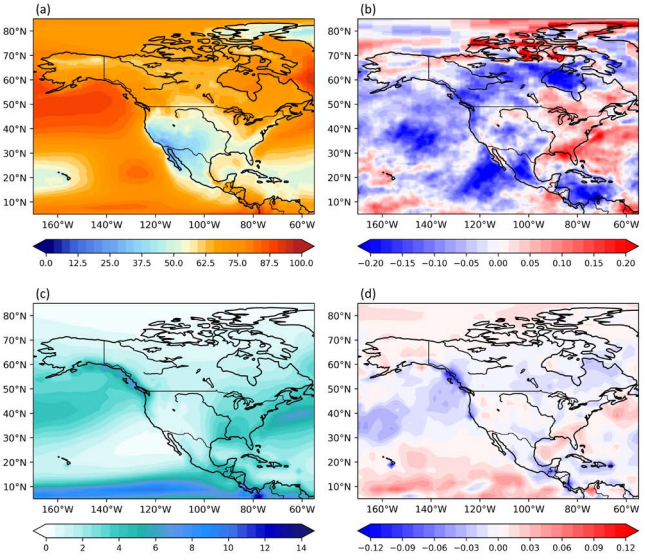

Fig 4. Climatology of (a) the average monthly means of cloud cover (unit: %) and (c) rate of precipitation (unit: mm/day) in NA from 2000 to 2023. The trend of (b) cloud cover (unit: % /year) and (d) rate of precipitation (unit: mm/day /year) in NA from 2000 to 2023. The trend is slope calculated by the simple linear regression.

Clouds and precipitation are closely related, and changes in one are believed to largely reflect changes in the other [24]. The low cloud cover on the NA West Coast resulted in reduced precipitation, which likely contributed to a degree of temperature increase. Conversely, high cloud cover on the East Coast led to greater precipitation, which may have partially mitigated temperature rise. Nonetheless, the effect of clouds and precipitation on the East and West Coasts does not align with the observed differences in warming rates between the two regions, indicating the presence of additional influencing factors.

3.3.2 Radiation

Combining Fig.5(a) and 5(d), it can be observed that the shortwave radiation received by the satellite exhibits a pattern of lower amounts and smaller decreases along the west coast, and higher amounts and larger decreases along the east coast. This indicates that there is not a significant difference in shortwave radiation between the two coasts, prompting us to analyze longwave radiation (Fig.5(b) and 5(e)). Fig.5(b) reveals that there is little difference in the long-wave radiation amounts received by the satellite between the two coasts. However, Fig.5(e) shows an increasing trend in long-wave radiation received by the satellite over the west coast, suggesting a reduction in the remaining longwave radiation of the Earth's atmospheric system. Conversely, a decreasing trend in long-wave radiation received by the satellite over the east coast indicates an increase in the remaining longwave radiation of the Earth's atmospheric system. These findings suggest that, with minimal differences in shortwave radiation between the two coasts, the decrease in long-wave radiation over the west coast leads to a downward trend in net radiation, while the increase in long-wave radiation over the east coast results in an upward trend in net radiation.

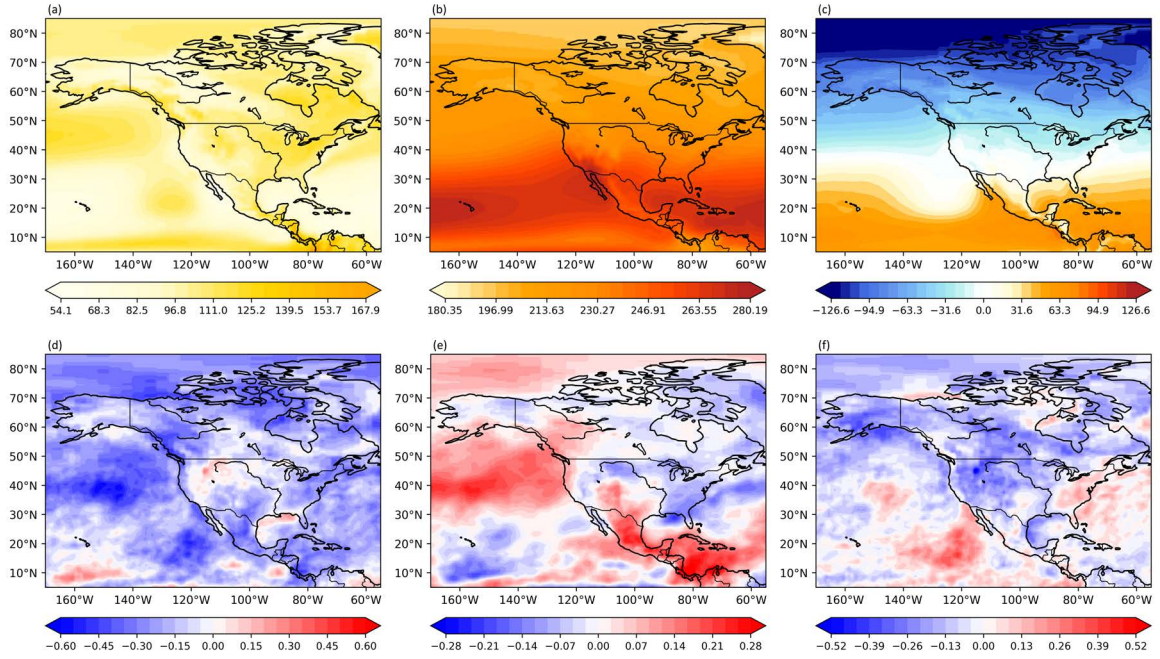

Fig 5. Climatology of the average monthly means of top of atmosphere (TOA) short-wave (a), long-wave (b), and net (c) flux (unit: W m^{-2}) in NA from 2000 to 2023; The trend of average monthly means of TOA short-wave (d), long-wave (e), and net (f) flux (unit: W m^{-2}/year) in NA from 2000 to 2023. The trend is the slope calculated by the simple linear regression. All the data is under the all-sky conditions.

Moreover, the trend map of net radiation for the Earth's atmospheric system (Fig.5(f)) shows that the results are consistent with previous deductions. It reveals a decreasing trend in net radiation for the west coast, which has a cooling effect on warming, and an increasing trend for the east coast, which promotes warming. This observation aligns with the phenomenon of slower warming rates on the west coast and faster warming rates on the east coast. It is noteworthy that, although the distribution map of net radiation for the Earth's atmospheric system (Fig.5(c)) shows small positive or even negative net radiation values on both coasts, this does not contradict the trend of rising temperatures. This discrepancy may be due to historically low average net radiation values in the region over an extended period, combined with other factors influencing the observed temperature increase.

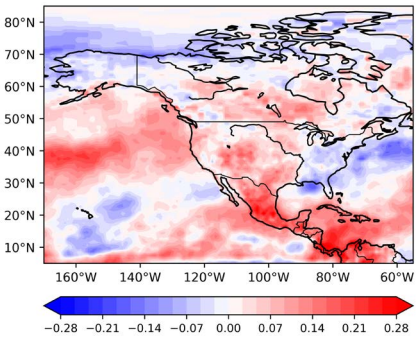

Fig 6. The trend of average monthly means of TOA long-wave flux (unit: W m^{-2}/year) in NA from 2000 to 2023. The trend is the slope calculated by the simple linear regression. The data is under the all sky minus clear sky conditions.

Fig.6 reveals that under the influence of clouds, the long-wave radiation received by satellites increases on the west coast while decreasing on the east coast. This observation is consistent with the results shown in Fig.5(e), further illustrating that clouds can affect longwave radiation on both coasts, thereby impacting the net radiation of the Earth's surface and ultimately leading to changes in temperature trends. However, analysis based solely on clouds, precipitation, and radiation does not explain why the central region of NA experiences the slowest rate of warming. Therefore, the subsequent discussion will address the effects of sea level pressure and wind.

3.3.3 Sea Level Pressure & Wind Circulation

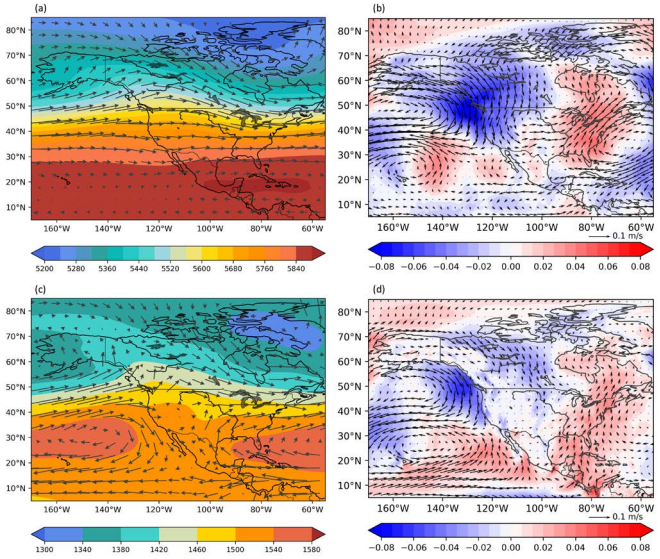

Fig.7 (a) The climatology (vector arrow, unit: m s^{-1}, shadings represents potential height, unit: gpm) and (b) the trend (vector arrow, unit: m s^{-1} /year, shadings represents strength of meridional wind trend, unit: m s^{-1} /year, southerly (northerly) wind is positive (negative), red(blue) color) of 500hPa and (c)850hPa upper wind field and (d) trend during the 2000-2023 period.

As shown in Fig.7(a), mean wind field is dominated by zonal westerly wind in the high level, where there is no many differences between west and east coast. However, Fig.7(b) shows a northerly wind trend in the west coast and middle, southerly wind trend in the east coast. These trends are strong both in 500hPa and 850hPa level (Fig.7(b) and 7(d)), which would generate a "wave"-like wind field (Fig.7(a) and 7(c)). Northerly wind trend brings more cold air from the North Pole to the centre, which makes a cooling effect for forming a "warm hole" in the midland. On the contrary, Southerly wind trend brings more warm and moist air from the Gulf of Mexico, which can cause a warming effect.

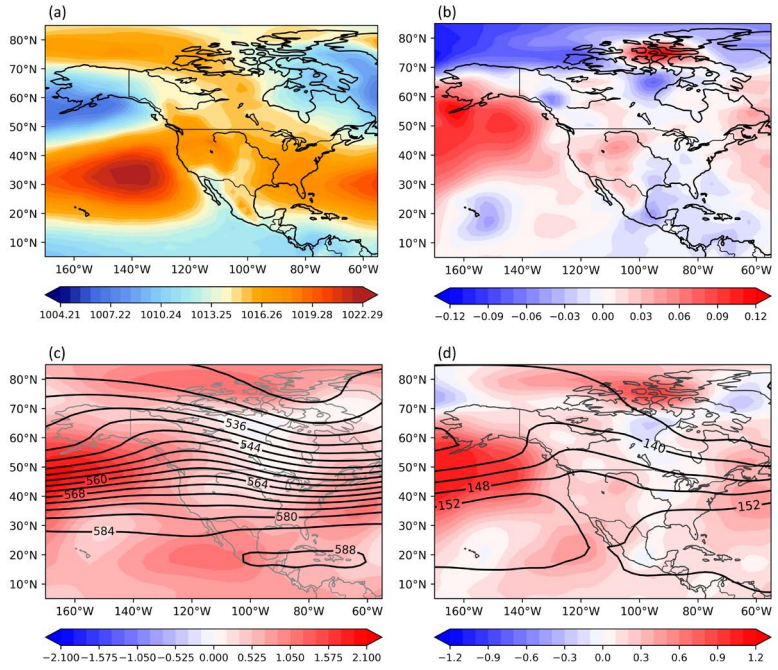

Fig.8 (a) The climatology (unit: hPa) and (b) trend (unit: hPa /year) of the sea level pressure, the climatology (solid black line, unit: gpm) and trend (shadings, unit: gpm /year) of the geopotential height in (c)500hPa and (d)850hPa.

Combined with the geopotential height climatology and trend of 500hPa and 850hPa (Fig.8(c) and 8(d)), it can be seen that the position of the upper level high centre of 500hPa corresponds to a surface low pressure centre (Fig.8(a)). Since the trend is positive (shadings in Fig.8(c)), the high centre of the upper level will strengthen. As the west coast is located on the eastern edge of the strengthening high pressure centre, an anticyclone anomaly will be generated locally, so the winds on the west coast and the central region will have a northerly trend. In particular, the central region is between abnormally decreasing and increasing sea level pressure (Fig.8(b))at surface, so there will be abnormal northwest winds, bringing more cold air. At the same time, the east coast, as the western margin of low pressure decline, has abnormal positive pressure, and the wind field presents a southerly trend. The near surface is also between abnormally high and low sea level pressure (Fig.8(b)), blowing southerly winds that bring a lot of warm air over the ocean.

3.3.4 Correlation Analysis

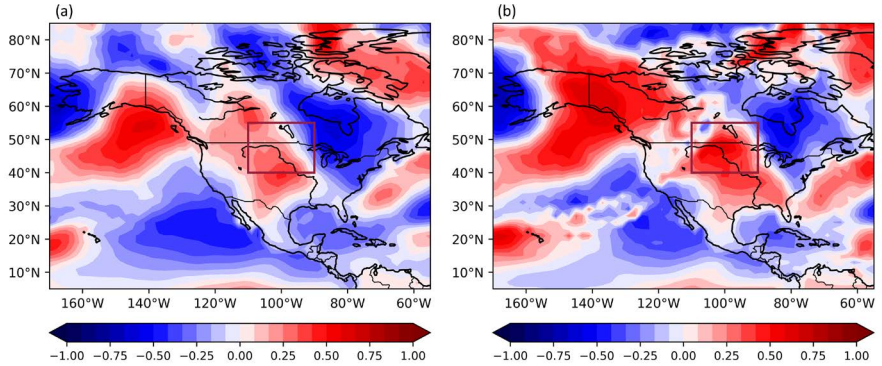

Fig.9 Pearson correlation coefficient distribution of (a)850hPa and (b) 500hPa wind field with temperature (positive/negative correlation is red/blue).

To explore the extent to which radiation and wind field effects play a role in local temperature trends over the west, central, and east coast of NA, we performed correlation analysis using Pearson correlation coefficients (range -1 to 1). The results show that for the annual mean temperature, the correlation between the meridional wind field and

temperature at 850hPa height is relatively high (positive) in the central region of NA (Fig.9(b)). If we analyze the correlation between the regional mean temperature and the meridional wind field in the central region (110°W~ 90°W, 40°N~ 55°N), the Pearson correlation coefficient will reach 0.55. This indicates that the near-surface wind field has affected the temperature change in the central part of NA to some extent, and the abnormal north wind in the past 24 years will cause the temperature in the central part of NA to drop through the cold air transported to the south.

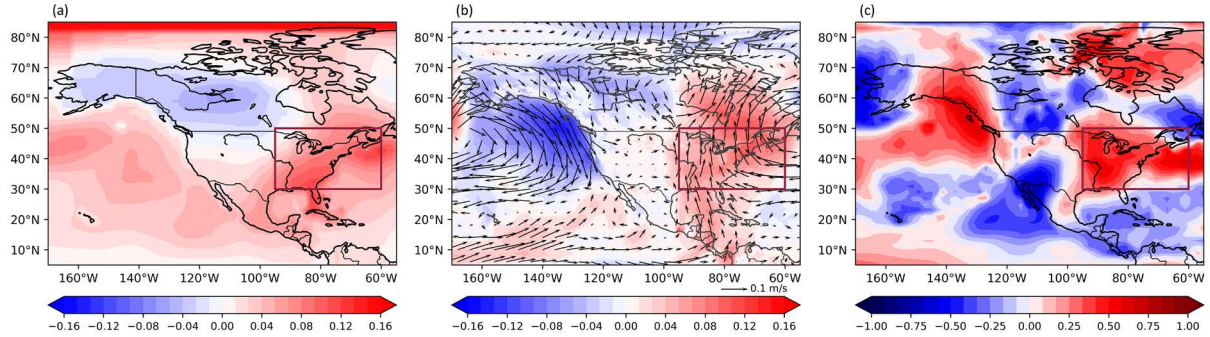

Fig.10 Analysis of temperature influencing factors on the East Coast (focusing on winter). (a) The trend of winter temperature (unit: K/year). (b) 500hPa wind field (shadings, unit: gpm / year, South (North) wind is positive (negative), red (blue) color fill). (c) The distribution of the Pearson correlation coefficient of the 500hPa (positive (negative) correlation is in red (blue).

For the east coast, the correlation between the wind and the whole year is not obvious, even a small part is negative, which may be the influence of the wind field is only affected in a certain season. So if we make a correlation directly using year-round data, it will be affected by other seasonal disturbances, and in this study we have been able to take the winter to discuss it separately. The study found that in winter, meridional wind had a more significant correlation with temperature in the east coast at the 850hPa. The average temperature of the winter average and the winter longitude of the eastern coast(95°W~60°W,30°N~50°N) were analyzed by correlation analysis, Pearson correlation coefficient is 0.38. At the same time, the significant increase of temperature trend in winter on the east coast (Fig.10(a)) and the significant southerly wind trend of the winter (Fig.10(b), red color filled) can be determined, the abnormal southerly wind in winter brought the warm and wet air of the gulf of Mexico to lead to the rise of temperature in the east coast, and thus made a positive contribution to the distribution of annual temperature trends on the east coast (Fig.3(b), compared to the west coast and the central region, the east coast has largest trend).

In the western region, the relationship between the wind and cooling is less obvious and even negative (Fig.9(a) and 9(b)), which means that the north wind is not entirely associated with the cooling effect on the west coast, and the north wind may have a warming effect. This may be because the north coast of North America is different from the central region, the north of the west coast is not necessarily cold air. Because it is located on the east side of the anti-cyclone wind field, it may be affected by the air flow from the ocean area (which may be heated by seawater), or because of its terrain (including the codilla and the Rocky Mountains), there may be some undiscovered mechanisms that are more complex.

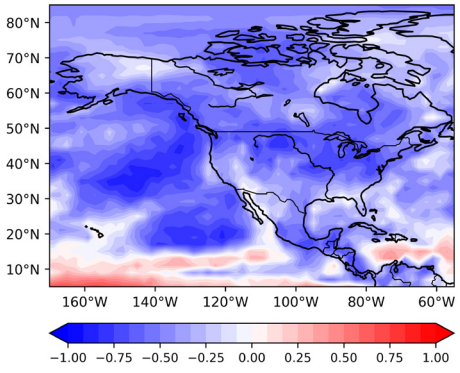

Fig.11 Trends in shortwave radiation since the 21st century (unit: W m^{-2} /year)

About the effects of radiation fields, there is a strong correlation between shortwave radiation received by satellites and temperature change (Fig.11). In other words, the downward trend of shortwave radiation received by satellites will lead to a trend of temperature rise, which suggests that it may be the cause of the growth trend in the west coast region. If we use the regional average temperature of west coast area(130°W~110°W,25°N~55°N), the correlation coefficient of the sea wavelength is analyzed, and the coefficient of the Pearson is -0.74. The linear fitting line determines the coefficient of R-squared is 0.55.

There is no other warming effect has been found to warm the west coast.

Above all, the wind field and radiation have a certain effect on the temperature growth trend in NA. The trend of the wind field often reflects the regional differences in the trend of temperature change. The influence of the wind field throughout the year is concentrated in the middle of the NA, which is affected by the northerly wind from the north pole, and promotes the cooling trend in the central region, which makes the central region heat up slowest. The winter wind field has a certain increase in the region of the NA east coast (the unusually southern wind brings the Gulf of Mexico air), and the west coast region is mainly affected by the trend of the shortwave radiation.

4. Conclusion

The rise in temperature on the west and east coast of NA in the 21st century has been different for various factors, including the slowest rise in temperatures in central NA, and there seems to be a hole. The study found that the radiation field and the wind field had an effect on the temperature growth trend of the research area. In the whole year, under the influence of the regional differences in the cloud, the increase of long wave radiation (received by satellites) in the west coast and the decrease in the east coast, affects the difference between the overall increase in the two regions, precipitation under the influence of clouds has little effect on it. The abnormal effect of the wind field is one of the cooling and warming mechanisms, and the regional differences in the trend of temperature change are also reflected. Year-round northerly wind anomaly has been affecting the temperature of the central region, which has cooled by cold air from the North Pole. The winter wind field has a certain increase southerly trend in the eastern coastal region, which brings the Gulf of Mexico warm and wet air, making the east coast region warmer in the past year. For the west coast's warming mechanism, it may be modulated by some unknown air-sea interaction mechanisms, and it may be affected by short-wave radiation.

There are many uncertainties derived from the satellite data and the limitations of the re-analysis data itself objectively, but these uncertainties are accepted. If there are longer time scale data in the future, we will continue to improve the current work and strive to find more influence factors to improve the formation mechanism of uneven temperature rise distribution under climate warming.

The future should further study the mechanism of temperature change in the west coast region, especially the factors affecting the ocean or terrain, and the seasonal differences that affect different factors in different regions, and the interconnections between different influencing factors. If the internal feedback mechanism can be found, it will be beneficial to study the causes and effects of the increase in temperature rise in the area.

Acknowledgement

Ruyun Xie, Yunbo Zhao, and Xinlin Ni contributed equally to this work and should be considered co-first authors.

References

[1] Hicke et al., "North America. In: Climate Change 2022: Impacts, Adaptation and Vulnerability. Contribution of Working Group II to the Sixth Assessment Report of the Intergovernmental Panel on Climate Change [H.-O. Pörtner, D.C. Roberts, M. Tignor, E.S. Poloczanska, K. Mintenbeck, A. Alegría, M. Craig, S. Langsdorf, S. Löschke, V. Möller, A. Okem, B. Rama (eds.)]," Cambridge University Press, Cambridge, UK and New York, NY, USA, pp. 1929–2042, 2022.

[2] G. A. Meehl, C. Tebaldi, and D. Adams-Smith, "US daily temperature records past, present, and future," Proceedings of the National Academy of Sciences of the United States of America, vol. 113, no. 49, pp.13977–13982, 2016.

[3] K. E. Kunkel, D. A. Robinson, S. Champion, X. Yin, T. Estilow, and R. M. Frankson, "Trends and Extremes in Northern Hemisphere Snow Characteristics," Current Climate Change Reports, no. 2, pp. 65–73, 2016.

[4] M. Zemp et al., "Global glacier mass changes and their contributions to sea-level rise from 1961 to 2016," Nature, vol. 568, pp. 382–386, 2019.

[5] V. A. Alexeev, C. D. Arp, B. M. Jones, and L. Cai, "Arctic sea ice decline contributes to thinning lake ice trend in northern Alaska," Environmental Research Letters, vol. 11, no. 7, p. 74022–74023, 2016.

[6] J. Navarro-Estupiñan, A. Robles-Morua, E. R. Vivoni, J. E. Zepeda, J. A. Montoya, and V. S. Verduzco, "Observed trends and future projections of extreme heat events in Sonora, Mexico" International Journal of Climatology, vol. 38, no. 14, pp. 5168–5181, 2018.

[7] "IPCC, 2021: Climate Change 2021: TTe Physical Science Basis. Contribution of Working Group I to the Sixth Assessment Report of the Intergovernmental Panel on Climate Change [Masson-Delmotte, V., P. Zhai, A. Pirani, S.L. Connors, C. Péan, S. Berger, N. Caud, Y. Chen, L. Goldfarb, M.I. Gomis, M. Huang, K. Leitzell, E. Lonnoy, J.B.R. Matthews, T.K. Maycock, T. Waterfield, O. Yelekçi, R. Yu, and B. Zhou (eds.)]," Cambridge University Press, Cambridge, United Kingdom and New York, NY, USA, 2021.

[8] Z. Pan, R. Arritt, E. Takle, W. Gutowski, C. Anderson, and M. Segal, "Altered hydrologic feedback in a warming climate introduces a "warming hole," Geophys. Res. Lett., vol. 31, p. L17109, 2004.

[9] H. Ritchie, P. Rosado, and M. Roser, "CO_2 and Greenhouse Gas Emissions," Our World in Data, 2020.

[10] W. A. Robinson, R. Ruedy, and J. E. Hansen, "General circulation model simulations of recent cooling in the east-central United States," Journal of Geophysical Research: Atmospheres, vol. 107, no. D24, p. ACL 4–1–ACL 4–14, 2002.
[11] K. E. Kunkel, X.-Z. Liang, J. Zhu, and Y. Lin, "Can CGCMs Simulate the Twentieth-Century "Warming Hole" in the Central United States?," Journal of Climate, vol. 19, pp. 4137–4153, 2006.
[12] Q. Tang and G. Leng, "Changes in Cloud Cover, Precipitation, and Summer Temperature in North America from 1982 to 2009," J. Climate, vol. 26, no. 5, pp. 1733–1744, 2013.
[13] M. Wild, A. Ohmura, H. Gilgen, and D. Rosenfeld, "On the consistency of trends in radiation and temperature records and implications for the global hydrological cycle," Geophys. Res. Lett., vol. 31, p. L11201, 2004.
[14] J. Shinker and P. J. Bartlein, "Visualizing the Large-Scale Patterns of ENSO-Related Climate Anomalies in North America," Environmental Science, Geography · Earth Interactions, vol. 13, 2009.
[15] N. G. Loeb et al., "Clouds and the Earth's Radiant Energy System (CERES) Energy Balanced and Filled (EBAF) Top-of-Atmosphere (TOA) Edition-4.0 Data Product," J. Climate, vol. 31, no. 2, pp. 895– 918, 2018.
[16] S. Kato et al., "Surface irradiances of Edition 4.0 Clouds and the Earth's Radiant Energy System (CERES) Energy Balanced and Filled (EBAF) data product," J. Climate, vol. 31, no. 11, pp. 4501–4527, 2018.
[17] R. F. Adler et al., "The Global Precipitation Climatology Project (GPCP) monthly analysis (new version 2.3) and a review of 2017 global precipitation," Atmosphere, vol. 9, no. 4, pp. 138–139, 2018.
[18] Lenssen et al., "Improvements in the GISTEMP uncertainty model," J. Geophys. Res. Atmos, vol. 124, no. 12, pp. 6307–6326, 2018.
[19] Hansen, J., R. Ruedy, M. Sato, and K. Lo, "Global surface temperature change," Rev. Geophys, vol. 48, no. 4, 2010.
[20] Vose, R.S., D. Easterling, K. Kunkel, A. LeGrande, and M. Wehner, "Temperature changes in the United States," Climate Science Special Report: Fourth National Climate Assessment, vol. 1, pp. 185–206, 2017.
[21] L. R. Mudryk, J. Dawson, S. E. L. Howell, C. Derksen, T. A. Zagon, and M. Brady, "Impact of 1, 2 and 4 °C of global warming on ship navigation in the Canadian Arctic," Nature Climate Change, vol. 11, pp. 673–679, 2021.
[22] Greenan et al., "Changes in oceans surrounding Canada; Chapter 7 in (eds.) Bush and Lemmen, Canada's Changing Climate Report," Government of Canada, Ottawa, pp. 343–423, 2018.
[23] Zhang et al., "Changes in Temperature and Precipitation Across Canada; Chapter 4 in Bush, E. and Lemmen, D.S.," Canada's Changing Climate Report. Government of Canada, Ottawa, Ontario, pp. 112–193, 2019.
[24] R. W. Portmann, S. Solomon, and G. C. Hegerl, "Spatial and seasonal patterns in climate change, temperatures, and precipitation across the United States," Proc Natl Acad Sci U S A., vol. 106, no. 18, pp. 7324– 7329, 2009.
[25] Hersbach et al., "ERA5 monthly averaged data on pressure levels from 1940 to present," Copernicus Climate Change Service (C3S) Climate Data Store (CDS), 2023, doi: 10.24381/cds.6860a573